17th World Conference on Earthquake Engineering, 17WCEE
Sendai, Japan - September 13th to 18th 2020

Retrofit of masonry infills: local interaction with RC frames

G. Blasi [1], D. Perrone [2], M.A. Aiello [3], R. Fleischman [4]

[1] *Post-Doctoral Researcher, Department of Engineering for Innovation, University of Salento, Lecce, Italy,* gianni.blasi@unisalento.it

[2] *Post-Doctoral Researcher, University School for Advanced Studies IUSS Pavia, Pavia, Italy,* daniele.perrone@iusspavia.it

[3] *Full Professor, Department of Engineering for Innovation, University of Salento, Lecce, Italy,* antonietta.aiello@unisalento.it

[4] *Full Professor, Department of Civil and Architectural Engineering & Mechanics, University of Arizona, Tucson, USA* rfleisch@email.arizona.edu

Abstract

The achievement of code-based performance criteria in existing reinforced concrete buildings is often gained through different retrofit techniques aimed at improving the seismic behavior of both structural members and non-structural elements, such as infill walls. Focusing on masonry infill walls, state-of-art strengthening techniques are often adopted to increase the in-plane capacity and to prevent out-of-plane mechanisms. As stated by several studies, the interaction between the surrounding frame and the infill panels leads to a significant effect on the dynamic behavior of the structure and often modifies its collapse mechanism. Particularly when dealing with older buildings, the brittle failure of columns with poor transverse reinforcement can be triggered by the lateral forces transferred from the infill panel.

The influence of the retrofitting of the infill walls on the failure modes of buildings built prior to modern seismic provisions is investigated in this study. A numerical macro-model reproducing the lateral response of the strengthened panel has been developed. The numerical model is calibrated through experimental data and analytical formulations available in the literature. Non-linear static analyses are performed to assess the effect of the strengthening on the in-plane distribution of inertia forces and on the failure mode of the frames. The results represent a useful mean to assess the efficacy of the retrofit techniques that, despite reducing the damage to the masonry infills, can adversely affect the global performance of the RC frames in case of earthquake. Design recommendations are provided.

Keywords: Retrofitted infills, OpenSees, existing RC frames, Brittle failure, Seismic performances.

1. Introduction

The damage to reinforced concrete (RC) buildings due to earthquakes often involves failure of non-structural elements, as evidenced by the latest post-earthquake damage reports [1,2]. In the case of infill walls, in-plane and out-of-plane collapse might represent a severe risk for life-safety, even if the structure does not approach collapse. Physical tests [3,4] and numerical studies [5,6] of infilled RC frames conducted in recent years have highlighted the main vulnerability of masonry infill panels subjected to quasi-static and dynamic loading.

Masonry infill retrofit has been introduced in recent years in order to mitigate the non-structural losses, through techniques usually adopted for the strengthening in masonry buildings. The application of Fiber-Reinforced-Polymer (FRP) layers to the wall is aimed to increase the in-plane tensile strength and to prevent diagonal cracking [7]. Textile-Reinforced Mortar (TRM), Composite-Reinforced-Mortar (CRM) or Steel-Reinforced-Grout (SRG) jacketing lead to both higher lateral strength and higher stiffness [8].

Different analytical models are available in the literature, aimed at predicting the lateral response of strengthened masonry panels [9,10], with a particular focus on the shear strength. Gattesco and Boem [10] provided an amplification factor representing the ratio between the reinforced panel and the unreinforced panel strength, calibrated based on physical tests results of CRM strengthened walls. A formulation to predict the shear strength of masonry panels retrofitted with fiber-reinforced mortar was also provided by Cascardi et al. [9,11]. The authors used artificial neural networks to calibrate the formula, using a database of laboratory tests on different types of reinforced masonry walls.

The studies conducted in the past years led to a recent introduction of guidelines for retrofit techniques [12,13], which provide instruction for their design, installation and maintenance.

Despite the great effectiveness of these retrofit techniques from a seismic performance standpoint (e.g. increase of lateral strength of the masonry wall), it is worth considering that the enhancement of the mechanical performance of infill walls might significantly modify the structure's dynamics and failure modes. The global strength and stiffness of RC frames are indeed strongly influenced by the presence of the infill walls [14]. This issue is addressed in the building codes, which provide simplified formulations to encourage the assessment of the influence of the infill on the structural performance in practical design [15,16].

The analysis of the failure modes of infilled frames led to the definition of several models aimed at predicting the influence of the masonry panel on the seismic response of RC structures [17,18]. The latest numerical studies investigated the increase of the shear demand in the column due to the local interaction with the infill wall, demonstrating that strong panels might cause early failure of the columns [5,19].

The analysis of the local interaction between the infill wall and the surrounding frame is a matter of paramount importance in older (pre-code) RC buildings, since the frames are not detailed for seismic response Post-earthquake loss estimations indicated brittle failure modes of the columns due to the increase of the shear demand caused by the presence of the masonry infill panel [20].

This paper presents numerical results on the main effects of the retrofit of the infill masonry walls in pre-code buildings. A numerical macro model is developed in the OpenSees platform [21] to simulate the cyclic response of different types of RC frames. The failure modes of a bare frame, an unreinforced infilled frame and an infilled frame with a strengthened infill panel are compared to assess the effectiveness of the retrofit in terms of seismic performance. Furthermore, different strengthening techniques are considered, namely an FRP layer applied along the diagonal of the wall and a CRM jacketing. Non-linear cyclic pushover analyses are conducted to assess the failure modes of the frame members based on the infill properties. Using the obtained results, design recommendations that accurately reflect the effect of the retrofit on old existing infilled frames are provided, based on the properties of the wall and the frame members.

2. Description of the case study frames

In order to investigate the behavior of RC frames with retrofitted infill, three types of infilled portals were analyzed. Each considered system reproduced the configuration of the first floor in a 4-storey and 4-bay regular RC building designed for gravity loads. A simulated design of the frames was conducted, considering the usual configuration of Multi-storey RC buildings in Mediterranean regions.

The cross section of the columns was designed for axial load, according to the tributary area approach. The tributary area was calculated considering the in-plane and out-of-plane length of the slab, L, equal to 5.4 m. The longitudinal reinforcement of the column was defined as 1% of the cross-sectional area, according to the provisions of the Italian building code [22] The height of the cross-section of the beam was assumed equal to L/10. A continuous beam assumption was considered for the evaluation of the bending moment in the beam and, consequently, of the longitudinal reinforcement. The dead and live loads on the slab were assumed equal to 5.8 kN/m^2 and to 2.0 kN/m^2, respectively.

In Table 1, a description of the analyzed frames is provided. An identification code is assigned to each frame depending on the retrofit technique assigned (URF = Frame with UnReinforced infill; FRPF = Frame with Fiber-Reinforced-Polymer infill; CRMF = Frame with Composite-Reinforced-Mortar jacketing of the infill).

Table 1 – ID of the case study frames

Frame ID	Column cross section [mm]	Beam cross section [mm]	Infill thickness [mm]	Retrofit type
URF	400x400	400x500	200	none
FRPF	400x400	400x500	200	FRP Layer
CRMF	400x400	400x500	200	CRM jacket

The configuration of the analyzed portals is illustrated in Fig. 1. The properties of the infill wall were defined basing on the usual configuration adopted in the Mediterranean regions, as well as the results of physical tests available in the literature [23,24]. The shear strength, τ_w, and the compressive strength, f_{cw}, were assumed equal to 0.15 MPa and 4 MPa, respectively, while the elastic modulus E_w and the shear modulus G_w were equal to 1200 MPa and 300 MPa, respectively.

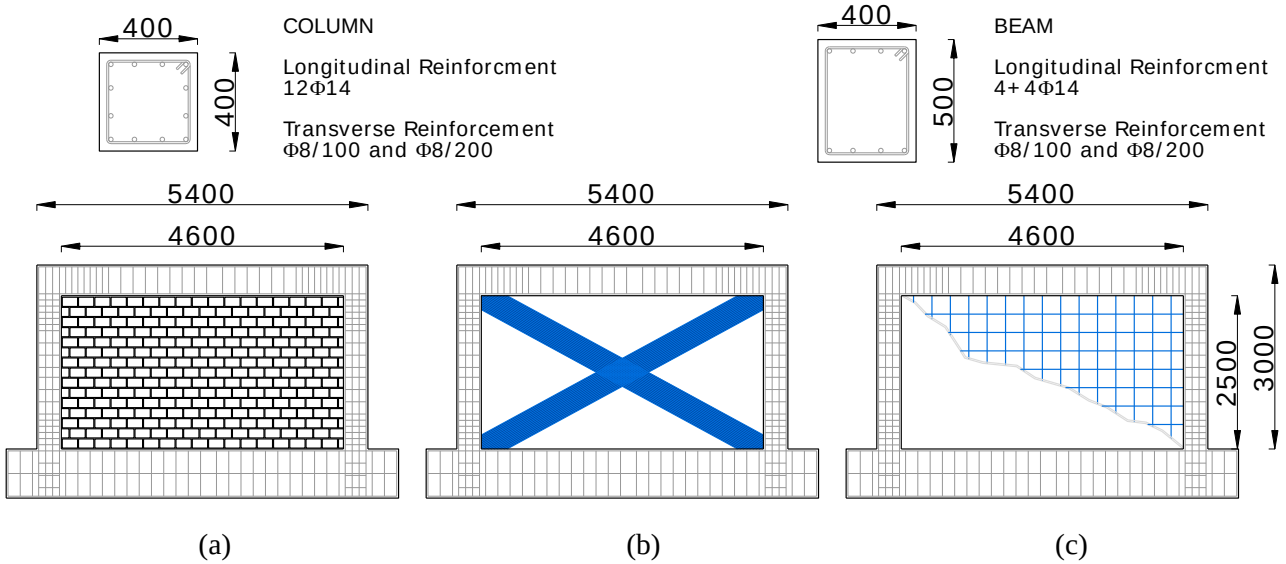

Fig. 1 – Configuration of the case study frames: (a) URF; (b) FRPF; (c) CRMF

The FRP retrofit features carbon-fiber composite sheet with equivalent thickness, t_f, equal to 0.169 mm and width, b_f, equal to 400 mm, applied along the diagonal of the wall (Fig. 1b). The tensile strength, f_f, and the elastic modulus E_f were equal to 3150 MPa and 270 GPa, respectively.

The CRM jacketing is composed of a 990x990 mm glass fiber mesh grid with cementitious matrix, having total thickness equal to 25 mm and compressive strength equal to 5 MPa. The tensile strength f_f and the equivalent thickness t_f of the fiber grid were equal to 1400 MPa and 0.02 mm, respectively.

The design of the FRP and the CRM retrofit was conducted by the definition of a target shear strength of the wall, F_{hw}, calculated based on the seismic base shear demand, F_h. The value of F_h was calculated according to the equivalent static approach described in the Italian building code [22] considering the equation (1):

$$F_h = \frac{S_a(T_1) \cdot \lambda \cdot W_b}{q_b} \tag{1}$$

where W_b and q_b are the weight and the behavior factor of the building, respectively, λ is the participating mass coefficient, equal to 0.85, and $S_a(T_1)$ is the spectral acceleration corresponding to the first period of the structure.

The behavior factor of the building was assumed equal to 1.5, representing the dissipation capacity of pre-code buildings. The value of $S_a(T_1)$ was defined referring to design spectrum evaluated for a high seismic hazard zone in Italy and for a return period equal to 475 years, as prescribed in the Italian building code for residential buildings [22].

For each orthogonal direction of the lateral seismic action, the base shear was distributed among the RC columns and the infill walls, based on the lateral stiffness of each element. Therefore, the value of F_{hw} was computed as $F_{hw}=\alpha_w \cdot F_h/[n_w \cdot (\alpha_w+1)]$, being α_w the infill-to-frame relative elastic stiffness and n_w is the number of infill walls in the considered direction. The value of α_w was calculated according to the equation:

$$\alpha_w = \frac{n_w G_w t_w l_w h_c^3}{n_c 12 E_c I_c h_w} \tag{2}$$

In the equation (2), n_c is the number of columns oriented in the considered direction; t_w, l_w and h_w are the thickness, the length and the height of the infill wall, respectively, G_w is the shear modulus of the masonry, E_c, I_c and h_c are the elastic modulus of the concrete, the moment of inertia of the cross section and the height of the columns, respectively.

Depending on the strengthening technique considered, two different models were adopted to evaluate the lateral strength of the retrofitted wall. In the case of CRM jacketing, the equation proposed by Cascardi et al. [11] was used, which provides the global shear strength of the infill as function of the cross section, A_w, the compressive strength of the masonry, f_{cw}, the contribute to the shear strength provided by the composite fiber, $F_{f,CRM}$ and by the matrix, F_{matrix}:

$$F_{CRM} = \alpha f_{cw}^{0.5} \cdot A_w + F_{f,CRM} + F_{matrix} \tag{3}$$

where α is a parameter dependent on the tensile strength of the composite fiber and of the masonry, as well as on the compressive strength of the matrix and of the masonry (further details are provided in [9,11]).

In the case of FRP layers, the shear strength of the retrofitted panel was obtained by the equation:

$$F_{FRP} = \tau_w \cdot A_w + F_{f,FRP} \tag{4}$$

where τ_w is the shear strength of the masonry and $F_{f,FRP}$ is the contribution to the shear strength provided by the composite fiber.

The value of $F_{f,FRP}$ was computed according to the formulation provided in CNR-DT 200/2013 [13]:

$$F_{f,FRP} = 0.48 \cdot l_w \cdot 2t_f \cdot \sqrt{\frac{2 \cdot E_f \cdot \Gamma_F}{t_f}} \quad (5)$$

where $A_{f,FRP}$ E_f, t_f and Γ_f are the elastic modulus, the thickness and the fracture energy of the composite fiber layer, respectively. In Table 2, the properties of the infill retrofit, are provided.

Table 2 – Infill wall retrofit details.

Frame ID	Fiber material	Matrix thickness [mm]	Fiber's minimum Tensile strength [MPa]	Minimum Young's Modulus [GPa]
FRPF	Carbon	--	3150	270
CRMF	Glass	25	1400	25

3. Numerical modelling of the case study frames

The masonry infilled frames were modelled in OpenSees [21] according to different approaches, depending on the considered retrofit technique.

A fiber-based distributed plasticity model was used to simulate the non-linear flexural response of the RC frame members. Additionally, lumped non-linear springs (Fig. 2) were included at the ends of the columns, aiming to reproduce the brittle shear failure due to the interaction with the infill walls.

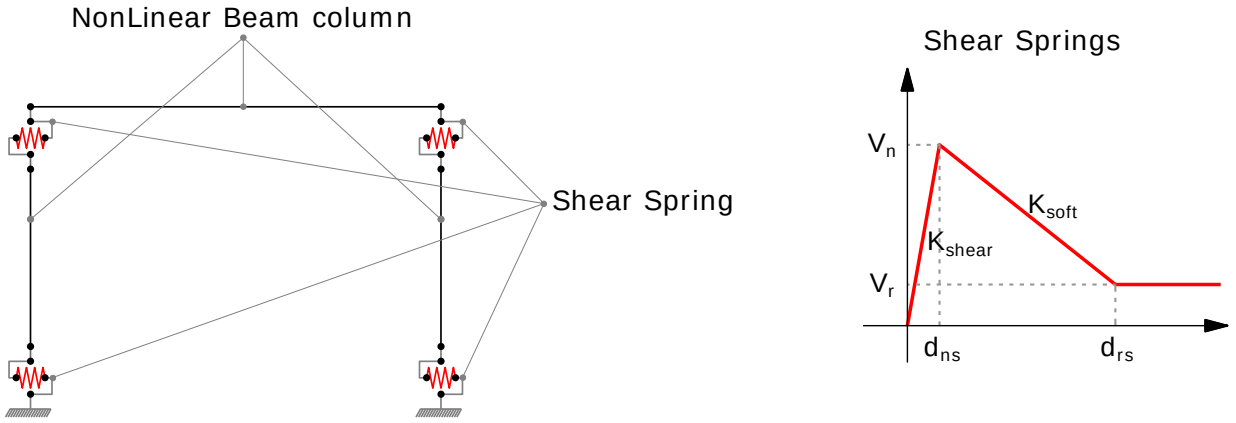

(a) (b)

Fig. 2 – Numerical modelling of the RC frames: (a) Discretization; (b) Shear Spring Backbone Curve.

The shear springs featured a bi-linear softening behavior with peak shear strength V_n, computed according to Sezen and Moehle [25]. The elastic and the softening slope were equal to $K_{shear} = G_c \cdot A_c / h_c$ and $K_{soft} = -0.8 K_{shear}$, respectively, where G_c is the shear modulus of the concrete, and A_c is the column cross-sectional area.

The presence of the masonry infill was simulated by including a three-diagonal strut system, which provides a reasonable representation of the additional shear demand in the column due to the presence of the wall [26]. The total width of the strut system was calculated as $b_w = 0.175 \cdot \lambda_h \cdot h^{-0.4} \cdot d_w$, according to Mainstone [27], as a function of the masonry panel diagonal dimension, d_w, and the panel-to-frame relative cracked stiffness, λ_h.

The equation (6) provided by Stafford Smith and Carter [28] was used to estimate λ_h, where θ_w is the angle of the wall diagonal with respect to the horizontal, and E_w is the equivalent elastic modulus of the wall.

$$\lambda_h = \sqrt[4]{\frac{E_w t_w sin(2\theta_w)}{4E_c I_c h_w}} \tag{6}$$

The force-displacement relationship of the unreinforced masonry wall was defined by adopting the tri-linear behavior proposed by Panagiotakos and Fardis [29], as shown in Fig. 3a. The cracking strength and the peak lateral strength of the panel were estimated as $\boldsymbol{F_{cr}}=\boldsymbol{A_w}\cdot\boldsymbol{\tau_w}$ and $\boldsymbol{F_m}=1.44\cdot\boldsymbol{F_{cr}}$, respectively, according to Blasi et al. [5]. The elastic slope $\boldsymbol{K_1}$, and the secant slope, $\boldsymbol{K_2}$, representing the shear stiffness of the panel and the axial stiffness of the strut, are calculated as $\boldsymbol{G_w}\cdot\boldsymbol{A_w}/\boldsymbol{h_w}$ and $\boldsymbol{E_w}\cdot\boldsymbol{b_w}\cdot\boldsymbol{t_w}/\boldsymbol{d_w}$, respectively.

The behavior of each strut element in the numerical model was defined by assigning 50% of the total stiffness to the central strut (Truss A in Fig. 3) and the remaining 25% to each off-diagonal struts (Truss B in Fig. 3a). The off-diagonal trusses were connected to the columns and the beams at a distance from the joints equal to $\boldsymbol{z_c}$ = $0.75b_w/2\cos\theta_w$ and $\boldsymbol{z_b}$ = $0.75b_w/2\sin\theta_w$, respectively.

In the case of FRP retrofit of the masonry wall, a non-linear tie element was included in the numerical model, with axial peak strength and elastic stiffness equal to $\boldsymbol{F_{f,FRP}}$ and $\boldsymbol{K_{1FRP}}=\boldsymbol{E_f}\cdot\boldsymbol{A_f}/\boldsymbol{d_w}$ respectively. The post-peak softening slope, $\boldsymbol{K_{2FRP}}$, was assumed equal to the elastic stiffness, aiming to simulate the brittle failure of the carbon-fiber composite (Fig. 3).

The presence of the CRM retrofit was simulated by modifying the force-displacement behavior of the three-strut system. The peak elastic strength was equal to $\boldsymbol{F_{CRM}}$, while the elastic stiffness was increased to $\boldsymbol{K'_1}=\boldsymbol{G_w}\boldsymbol{A'_w}/\boldsymbol{h_w}$, in order to account for the higher thickness, t_w', of the strengthened wall. Additionally, the post-elastic behavior was defined by including a perfectly plastic slope ($\boldsymbol{F_m}$ = $\boldsymbol{F_{CRM}}$), according to the test results obtained by Gattesco and Boem [10]. After the attainment of the maximum displacement of the unreinforced infill, $\boldsymbol{d_m}$, the failure of the panel progressively reduces its contribution to the lateral strength. Therefore, the softening slope $\boldsymbol{K'_3}$ is assumed equal to $\boldsymbol{K_3}/2$, namely the average between the post-peak perfectly plastic slope and the softening slope of the unreinforced panel.

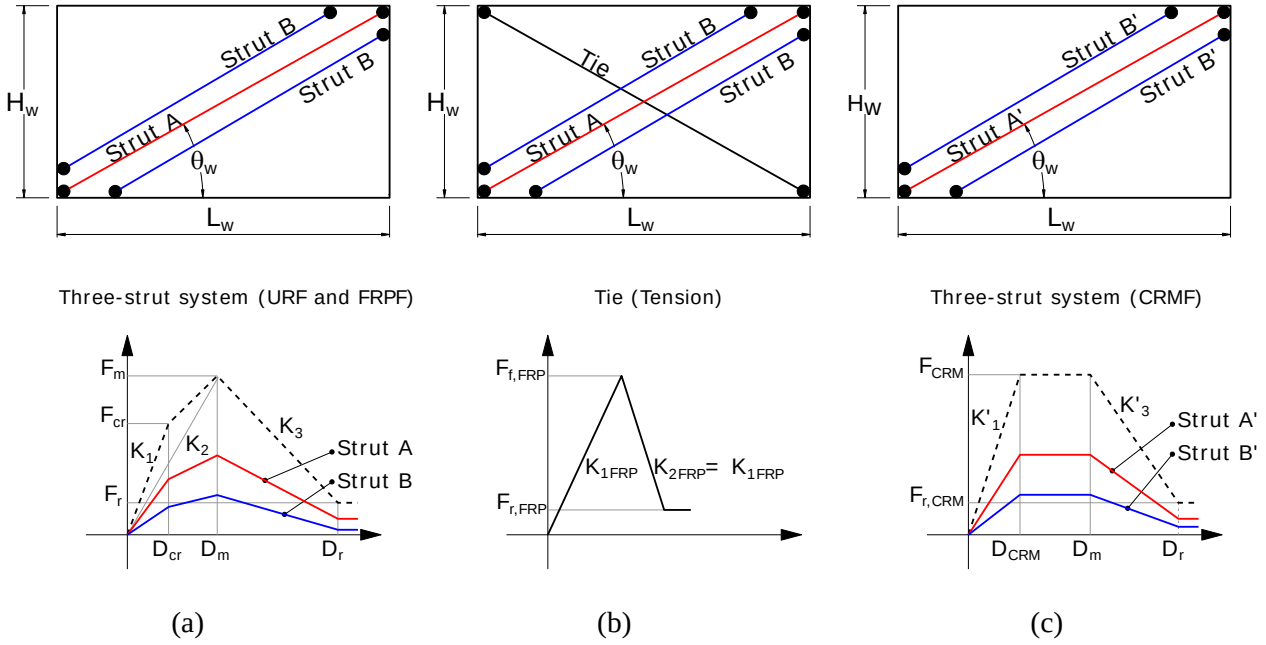

(a) (b) (c)

Fig. 3 – Numerical modelling of the masonry infill for (a) URF, (b) FRPF and (c) CRMF

4. Cyclic pushover analysis of the frames

A displacement-controlled load protocol was calibrated according to FEMA 461 [30], for the cyclic pushover analysis of the frames. Eight load steps were defined, each one was characterized by two full reversals of displacement. The displacement amplitude was increased by 40% at each step, up to the achievement of the maximum value Δ_{max}. The latter was calculated basing on ultimate chord rotation of the columns, $\theta_{u,c}$, according to equation (7), available in Eurocode 8 [31]:

$$\Delta_{max} = \theta_{u,c} \cdot h_c = 0.016 \cdot h_c \cdot (0.3^{\nu}) \left[\frac{max(0.01;\omega')f_c}{max(0.01;\omega)}\right]^{0.225} \left(\frac{L_v}{h_c}\right)^{0.35} 25^{\left(\alpha\rho_{sx}\frac{f_{yw}}{f_c}\right)} \quad (7)$$

In the equation, ν is the axial load ratio, ω and ω' are the reinforcement index for tensile and compressive longitudinal rebars, f_c is the cylindrical compressive strength of the concrete, L_v is the shear span, α is the confinement coefficient, ρ_{sx} and f_{yw} are the transverse reinforcement ratio and tensile strength, respectively.

Since the presence of the masonry infill wall generally reduces the displacement capacity of the RC frame, the value of Δ_{max} calculated by equation (7), could be fairly assumed as a upper limit for all the infilled frames analyzed. The zero-length springs in the columns (Fig. 2) allowed the brittle shear failure detection during the analysis, while the attainment of flexural failure was assessed in the post-processing basing on the stresses computed on the fiber sections.

In Fig. 4, the cyclic pushover results are provided for the infilled frames analyzed, in terms of hysteretic base shear-top displacement behavior. The significant influence of the infill retrofit is highlighted by the higher lateral strength, F_{max}, of FRPF and CRMF, which increased by 31% and 51%, respectively, with respect to URF.

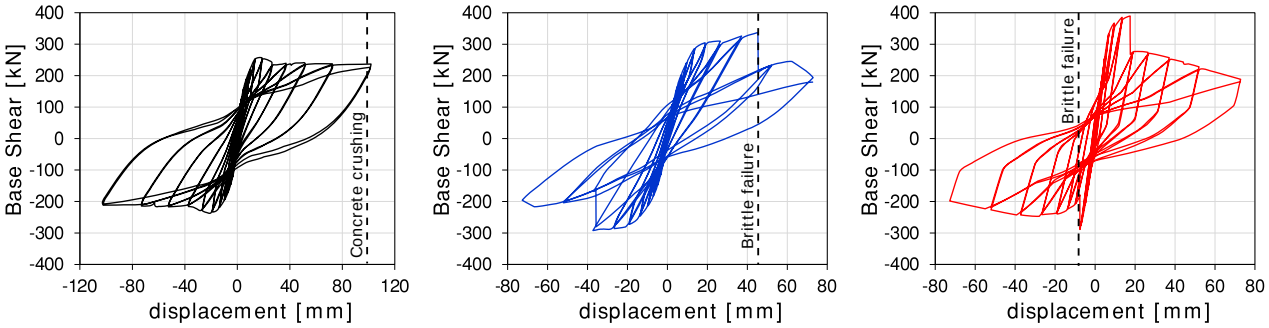

(a) (b) (c)

Fig. 4 – Hysteretic Base shear-displacement response obtained for (a) URF, (b) FRPF and (c) CRMF.

Although the infill wall strengthening modified the failure mode of the frames. A ductile failure was indeed obtained in the URF, featuring concrete crushing in the columns after longitudinal rebars yielding. For both CRMF and FRPF, brittle failure was observed, due to the attainment of shear failure of the columns.

In Fig. 5, the cumulative dissipated energy, ED, the ductility μ, and the displacement at failure FD, computed for each system, are reported. The values obtained were normalized to the result referred to URF, aiming to emphasize the effect of the infill retrofit.

A considerable reduction of the displacement capacity of the frames was observed in case of infill strengthening. For URF, the flexural failure was achieved at a top displacement equal to 99 mm, while the displacement at which the brittle failure occurred was equal to 46 mm and 7.6 mm for FRPF and CRMF, respectively.

Furthermore, the increase of the shear demand in the columns due to the infill retrofit reduced the ductility by 72% and 94% in FRPF and in CRMF, respectively, with respect to URF. A consistent fashion was observed regarding ***ED***, which reduced by 71% and 97% in FRPF and in CRMF, respectively, comparing to URF.

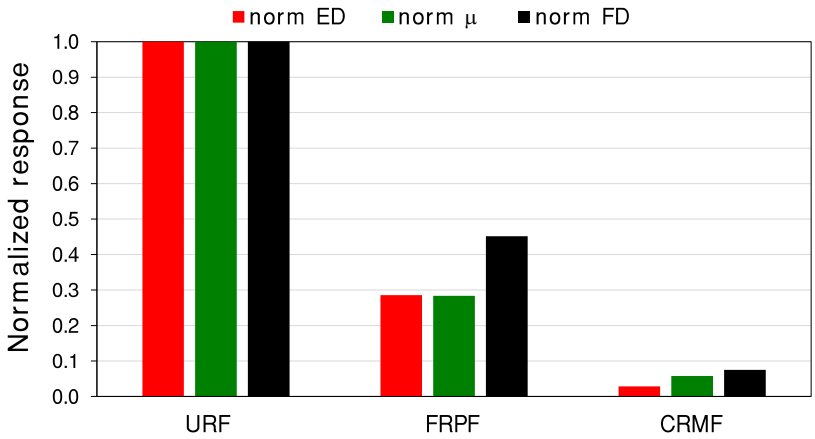

Fig. 5 – Normalized response obtained for the analyzed frames in terms of cumulative dissipated energy ***ED***, ductility μ, and failure displacement ***FD***.

5. Results discussion and design recommendations

Considering the lateral strength increase in the case of retrofitted infill, two additional simulations were carried out, for FRPF and CRMF. The new configurations analyzed (named FRPF' and CRMF') could be representative of RC portals featuring an FRP shear retrofit of the beam-column joints (e.g. according to [13]). The hysteretic response obtained for FRPF' and for CRMF' is provided in Fig. 6. In both cases, the higher strength of the column prevented the early brittle failure due to the interaction with the retrofitted infill wall. A ductile failure mode was observed, featuring concrete crushing after longitudinal rebars yielding, significantly increasing the displacement capacity of the frames.

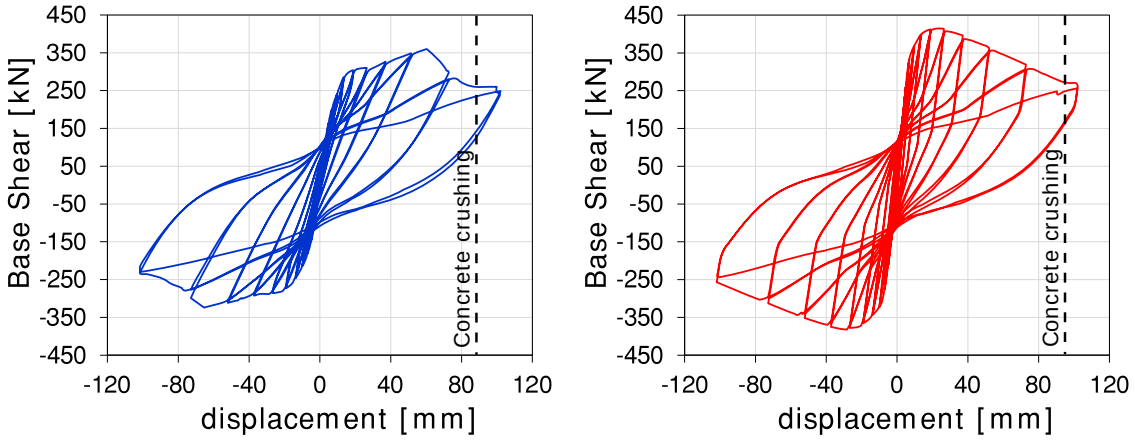

Fig. 6 – Hysteretic Base shear-displacement response obtained for (a) FRPF' and (b) CRMF'.

In Fig. 7, the updated results in terms of normalized ***ED***, μ and ***FD***, are provided. Referring to FRPF', a slight increase of the performance with respect to URF is observed. Composite-layer debonding on the infill wall occurred at a displacement amplitude equal to 60.8 mm. For this reason, the contribution of the retrofit to the energy dissipation capacity is not relevant. On the other hand, the FRPF' featured a significantly higher

performance compared to FRPF, due to ductile failure mode of the column and, consequently, to the higher displacement capacity.

In the case of CRMF', a noticeable increase of ***ED***, comparing to URF, was obtained. The higher lateral strength and the post peak-response of the retrofitted wall increased the area enclosed under the hysteretic loops. Although a slight decrease of the displacement capacity with respect to URF is observed also in this case, due internal forces increase and earlier concrete crushing. On the other hand, the greater elastic stiffness led to a significant increase of the ductility μ. The obtained results underline interesting and relevant aspects to consider at the design stage. In particular, the improvement of the seismic performance should always account for the frame-infill interaction; the strengthening may involve the frames, the infill walls or both, depending on the design target, as well as on the retrofit type.

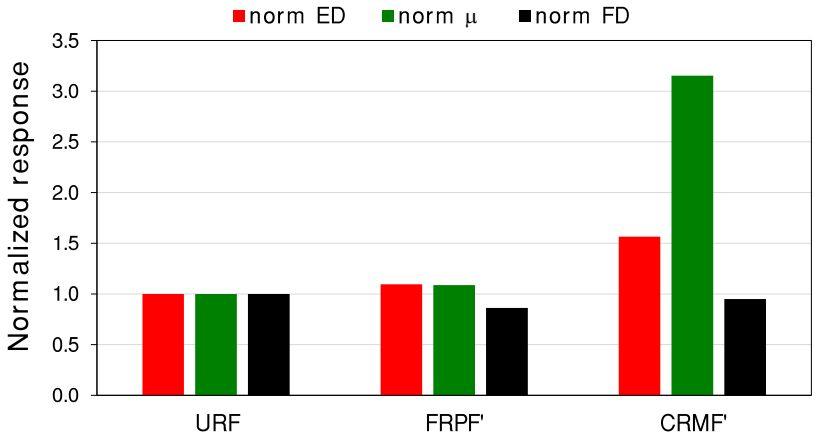

Fig. 7 – Normalized response obtained for URF, FRPF' AND CRMF' in terms of cumulative dissipated energy ***ED***, ductility μ, and failure displacement ***FD***.

6. Conclusions

The studies conducted in past years evidenced the seismic vulnerability of buildings designed prior to seismic provisions. Post-earthquake site inspections have documented masonry infill damage or collapse, which often represent a threat for life safety during seismic emergency. For this reason, the infill walls are often retrofitted to prevent both in-plane and out-of-plane failure in case of earthquake.

On the other hand, the retrofit of the masonry walls significantly increases their lateral strength and, consequently, the shear demand in the columns. Past studies evidenced a ductility decrease in RC frames due to brittle failure modes of the columns, as consequence of the interaction with strong infill walls. Therefore, a suitable design of the infill walls retrofit requires an accurate assessment of the failure mode of the frame, considering the influence of the strengthened infill.

In this study, the effect of the masonry infill retrofit on the seismic response of RC frames was investigated. The obtained results evidenced a major issue to be considered in the design of the masonry infill seismic retrofit. In the case of unreinforced infill, a ductile failure mode of the frame was obtained, while both retrofit techniques considered led to a significant reduction of the seismic performance. Despite the increase of shear strength caused by the retrofit, the early brittle failure of the column highly reduced the displacement capacity of the portals. The effect of the infill retrofit on the energy dissipation capacity was also evidenced by computing the ductility and the cumulative energy dissipated within the hysteretic cycles. A considerable reduction of the ductility was observed in the retrofitted portals due to the early brittle failure of the columns.

The analysis of the frames with strengthened beam-column joints evidenced the need of a comprehensive design of the infill retrofit. The sole infill strengthening (often realized to prevent the out-of-plane failure)

results indeed a suitable solution only in case of shear retrofit of the frame members, which avoids brittle failure.

Despite this study is focused on pre-code frames, the significant increase in wall strength, due to retrofit, suggests an influence on seismic designed frames' response, too. According to the capacity design, the shear demand on the column is generally evaluated depending on its flexural strength, while the increased demand due to the masonry infill wall is often neglected in practical design. The results provided in the present work represent a solid basis for the conduction of more accurate analyses, as well as physical tests on RC portals with retrofitted infills. Further studies would allow to improve existing design formulation for the retrofit of the masonry infill walls, accounting for the influence on the failure modes of the frame members.

ACKNOWLEDGEMENTS

This work was supported by "The Laboratories University Network of Seismic Engineering" (RELUIS) under Grant DPC-RELUIS 2019-2021.

References

[1] De Luca F, Woods GED, Galasso C, D'Ayala D (2017): RC infilled building performance against the evidence of the 2016 EEFIT Central Italy post-earthquake reconnaissance mission: empirical fragilities and comparison with the FAST method. *Bulletin of Earthquake Engineering*, 1–27.

[2] Ricci P, De Luca F, Verderame GM (2011): 6th April 2009 L'Aquila earthquake, Italy: Reinforced concrete building performance. *Bulletin of Earthquake Engineering*, **9** (1), 285–305.

[3] Kakaletsis D, Karayannis CG (2007): Experimental investigation of infilled r/c frames with eccentric openings. *Structural Engineering and Mechanics*, **26** (3), 231–50.

[4] Mehrabi AB, Shing PB, Schuller MP, Noland JL (1996): Experimental Evaluation of Masonry In-filled RC frames. *Journal of Structural Engineering*, **122** (3), 228–37.

[5] Blasi G, De Luca F, Aiello MA (2018): Brittle failure in RC masonry infilled frames: The role of infill overstrength. *Engineering Structures*, **177**, 506–18.

[6] Burton H, Deierlein G (2013): Simulation of Seismic Collapse in Non-Ductile Reinforced Concrete Frame Buildings with Masonry Infills. *Journal of Structural Engineering*, **140** (8), A4014016.

[7] Corradi M, Borri A, Castori G, Sisti R (2014): Shear strengthening of wall panels through jacketing with cement mortar reinforced by GFRP grids. *Composites: Part B*, **64**, 33–42.

[8] Vatani VO, Jafari A, Bazli M, Ghahri R (2018): Effect of different retrofitting techniques on in-plane behavior of masonry wallettes. *Construction and Building Materials*, **169**, 578–90.

[9] Cascardi A, Micelli F, Aiello MA (2016): Analytical model based on Artificial Neural Network for masonry shear walls strengthened with FRM systems Analytical model based on arti fi cial neural network for masonry shear walls strengthened with FRM systems. *Composites Part B*, **95**, 252–63.

[10] Gattesco N, Boem I (2015): Experimental and analytical study to evaluate the effectiveness of an in-plane reinforcement for masonry walls using GFRP meshes. *Construction and Building Materials*, **88**, 94–104.

[11] Cascardi A, Micelli F, Aiello MA (2017): Prediction of shear an compression strength of masonry structural elements rienforced by FRM (Fiber Reinfroced Moretar). *COST Action TU1207*, Budapest, Hungary.

[12] Consiglio Nazionale dell Ricerche (2018): *Istruzioni per la progettazione, l'esecuzione ed il controllo di interventi di consolidamento statico mediante l'utilizzo di compositi fibrorinforzati a matrice inorganica*. Italy.

[13] Consiglio Nazionale dell Ricerche (2014): *Istruzioni per la Progettazione, l'Esecuzione ed il Controllo di Interventi di Consolidamento Statico mediante l'utilizzo di Compositi Fibrorinforzati*. Italy.

[14] Perrone D, Leone M, Aiello MA (2016): Evaluation of the infill influence on the elastic period of existing RC frames. *Engineering Structures*, **123**, 419–33.

[15] FEMA 356 (2000): *FEMA 356 Prestandard and Commentary for the Seismic Rehabilitation of Building*. Federal Emergency Menagement Agency.

[16] ASCE/SEI 7-10 (2010): *Minimum Design Loads for Buildings and Other Structures*. American Society of Civil Engineers.

[17] Klingner RE, Bertero VV (1978): Earthquake resistance of infilled frames. *Journal of the Structural Division*, **104** (6), 973–989.

[18] Chrysostomou CZ, Gergely P, Abel JF (2002): A six-strut model for nonlinear dynamic analysis of steel infilled frames. *International Journal of Structural Stability and Dynamics*, **2** (3), 335–53.

[19] Stavridis A, Shing PB (2010): Finite-Element Modeling of Nonlinear Behavior of Masonry-Infilled RC Frames. *Journal of Structural Engineering*, **136** (3), 285–96.

[20] Parisi F, De Luca F, Petruzzelli F, De Risi R, Chioccarelli E (2012): *Field inspection after the May 20th and 29th 2012 Emilia-Romagna earthquakes*. Available at Http://Www.Reluis.It.

[21] McKenna F, Fenves GL, Scott MH, Jeremir B (2000): *Open system for earthquake engineering simulation, OpenSEES*. University of Berkeley.

[22] NTC-2018 (2018): *Aggiornamento delle «Norme tecniche per le costruzioni»*. D.M. 17 Gennaio 2018, Italy.

[23] Verderame GM, Ricci P, Del Gaudio C, De Risi MT (2016): Experimental tests on masonry infilled gravity- and seismic-load designed RC frames. *16th International Brick and Block Masonry Conference*, Padova (IT), p. 1349–58.

[24] Calvi GM, Bolognini D (2001): Seismic Response of Reinforced Concrete Frames Infilled With Weakly Reinforced Masonry Panels. *Journal of Earthquake Engineering*, **5** (2), 153–85.

[25] Sezen H, Moehle JP (2004): Shear Strength Model for Lightly Reinforced Concrete Columns. *Journal of Structural Engineering*, **130** (11), 1692–703.

[26] Chrysostomou CZ (1991): *Effects of degrading infill walls on the nonlinear seismic response of two-dimensional steel frames*. Cornell University.

[27] Mainstone RJ (1971): On the stiffnesses and strengths of infilled frames. *Proceedings of the Institution of Civil Engineers*, **49** (2), 57–90.

[28] Stafford Smith B, Carter C (1969): A method of Analysis for Infilled Frames. *Proceedings of the Institution of Civil Engineers*, **44** (1), 31–48.

[29] Panagiotakos TB, Fardis MN (1996): Seismic Response of Infilled RC Frame Structures. *11th World Conference on Earthquake Engineering*, Acapulco, Mexico.

[30] FEMA 461 (2007): *Interim Testing Protocols for Determining the Seismic Performance Characteristics of Structural and Nonstructural Components*. Federal Emergency Menagement Agency.

[31] EN 1998-3 (2005): *Eurocode 8: Design of structures for earthquake resistance - Part 3: Assessment and retrofitting of buildings*. European Standard.